IEEE Access
The journal for rapid open access publishing

IEEE Xplore Digital Library
http://ieeexplore.ieee.org/Xplore

Federated Learning in Vehicular Edge Computing: A Selective Model Aggregation Approach

DONGDONG YE[1,2], RONG YU[1,2], *Member, IEEE*, MIAO PAN [3], *Senior Member, IEEE*, and ZHU HAN [3], *Fellow, IEEE*

***Abstract*—Federated learning is a newly emerged distributed machine learning paradigm, where the clients are allowed to individually train local deep neural network (DNN) models with local data and then jointly aggregate a global DNN model at the central server. Vehicular edge computing (VEC) aims at exploiting the computation and communication resources at the edge of vehicular networks. Federated learning in VEC is promising to meet the ever-increasing demands of artificial intelligence (AI) applications in intelligent connected vehicles (ICV). Considering image classification as a typical AI application in VEC, the diversity of image quality and computation capability in vehicular clients potentially affects the accuracy and efficiency of federated learning. Accordingly, we propose a selective model aggregation approach, where "fine" local DNN models are selected and sent to the central server by evaluating the local image quality and computation capability. Regarding the implementation of model selection, the central server is not aware of the image quality and computation capability in the vehicular clients, whose privacy is protected under such a federated learning framework. To overcome this information asymmetry, we employ two-dimension contract theory as a distributed framework to facilitate the interactions between the central server and vehicular clients. The formulated problem is then transformed into a tractable problem through successively relaxing and simplifying the constraints, and eventually solved by a greedy algorithm. Using two datasets, i.e., MNIST and BelgiumTSC, our selective model aggregation approach is demonstrated to outperform the original federated averaging (FedAvg) approach in terms of accuracy and efficiency. Meanwhile, our approach also achieves higher utility at the central server compared with the baseline approaches.**

***Index Terms*—Federated learning, vehicular edge computing, model aggregation, contract theory.**

I. Introduction

FEDERATED learning has been proposed by Google as a distributed machine learning paradigm to push the computation of artificial intelligence (AI) applications into more and more end devices while protecting the privacy of end users [1]. In federated learning, a central server sends an initialized global deep neural network (DNN) model to clients as the first step. Based on the initialized global DNN model, clients separately train local DNN models with their local data as the second step. Instead of directly sending their local data, clients send the trained local DNN models back to the central server as the third step. The above steps are repeated in multiple rounds until the training accuracy of the global DNN model meets the requirement of the central server. Due to the above advantages, federated learning has been applied to many application scenarios, such as financial applications [1], virtual keyboard applications [2], and electronic health applications [3].

Vehicular edge computing (VEC) is a fast-developing vehicular technology, where vehicles and roadside servers at the network edge contribute communication, computation, storage and data resources to close proximity of vehicular users [4]. With the rapid penetration of intelligent connected vehicles (ICV), there is an urgent need to study federated learning in VEC as an important technical framework to meet the ever-increasing demands of AI applications in vehicular networks. In this paper, we consider image classification as a typical AI application in VEC [5]. As we know, the images captured from on-board cameras usually contain sensitive information with individual privacy of the vehicular clients. Using federated learning in VEC is beneficial in exploiting vehicular images for DNN training while protecting their privacy. For example, the vehicular clients use on-board cameras to capture images, which are classified and labeled by automatic labeling technology [6]. After that, the vehicular clients are selected by the central server to participate in federated learning in a supervised fashion and generate global and local DNN model updates.

The major challenge of federated learning in VEC is two folds. On the one hand, the diversity of image quality may cause severe loss of the accuracy of model aggregation. In VEC, the captured images generally suffer from motion blur, noise, and distortions [7], especially motion blur that is usually with different levels for different vehicular clients. During local training, the local DNNs are tuned according to the local images, and therefore, only work with the best accuracy under the specific statistics of the motion blur. As a result, the overall accuracy of the aggregated global DNN model will severely degrade if inappropriate local DNN models are involved. On the other hand, the diversity of computation capability has an

[1]School of Automation, Guangdong University of Technology, Guangzhou 510006, China
[2]Guangdong-HongKong-Macao joint Laboratory for Smart Discrete Manufacturing, Guangzhou 510006, China
[3]Department of Electrical and Computer Engineering, University of Houston, Houston, TX 77204, USA

This work of D. Ye and R. Yu was supported in part by program of NSFC under Grant 61971148, the Science and Technology Program of Guangdong Province under Grant 2015B010129001, Natural Science Foundation of Guangxi Province under Grant 2018GXNSFDA281013, Foundation for Science and Technology Project of Guilin City under Grant 20190214-3, and Key Science and Technology Project of Guangxi under Grant AA18242021. This work of M. Pan was supported in part by the U.S. National Science Foundation under Grants US CNS-1350230 (CAREER), CNS-1646607, CNS-1702850, and CNS-1801925. This work of Z. Han was supported in part by the US MURI AFOSR under Grants MURI 18RT0073, NSF EARS-1839818, CNS1717454, CNS-1731424, CNS-1702850, and CNS-1646607.

Corresponding author: Rong Yu (e-mail: yurong@ieee.org)

Digital Object Identifier: 10.1109/ACCESS.2020.2968399

impact on the efficiency of model aggregation. The difference in computation capability leads to different latency of training local DNN models. For synchronization, the central server performs model aggregation only after receiving all the local DNN models. This means that the vehicular clients with low computation capability hinder the efficiency of model aggregation [8].

To improve the accuracy and efficiency of model aggregation, this paper proposes a selective model aggregation approach. First of all, we exploit a geometrical model that illustrates the relationship between the object of interest and the camera in each vehicular client. The geometrical model is used to evaluate the image quality in the motion blur level by observing the instantaneous velocity of each vehicular client. After that, the computation capability is quantified via a parameter of resource consumption. By evaluating local image quality as well as computation capability, the "fine" local DNN models are selected and sent to the central server for aggregation. Since federated learning prevents from sending local data, the central server is not aware of the image quality and computation capability of vehicular clients, which is called information asymmetry. To deal with the information asymmetry, the selection procedure of the "fine" local DNN models is formulated as a two-dimensional image-computation-reward contract theory problem. The formulated problem is transformed into a tractable problem through relaxing and simplifying the complicated constraints, and eventually solved by a greedy algorithm. In summary, the main contributions of the paper are listed as follows.

- We study federated learning in VEC to meet the rapid-growing demands of AI applications in ICV. For federated learning with image classification, a selective model aggregation approach is proposed to reduce the influence from the diversity of image quality and computation capability in vehicular clients.
- A geometrical model that illustrates the relationship between the object of interest and the camera in each vehicular client is built up to evaluate the image quality in the motion blur level. According to the model, the image quality could be implicitly predicted by observing the instantaneous velocity of each vehicular client.
- To tackle the information asymmetry caused by federated learning, the model selection procedure is formulated as a two-dimensional contract theory problem. The problem is successively relaxed and simplified into a tractable problem, and solved by a greedy algorithm.
- Using the MNIST and BelgiumTSC datasets, the proposed selective model aggregation approach is shown to outperform the original federated averaging (FedAvg) approach in terms of the accuracy and efficiency of model aggregation. Also, our approach can achieve higher utility at the central server compared with existing baseline approaches.

The rest of this paper is organized as follows. Section II presents related work of federated learning in edge computing and distributed networks. Section III describes a general framework of federated learning in VEC. Section IV presents the system model for image quality, computation capability, vehicular client utility and type, and central server utility. In Section V, we describe contract formulation to the model selection procedure and elaborate the solution. Section VI shows performance evaluation and numeric results. Section VII gives conclusions of the paper.

II. Related Work

The challenging problem of federated learning in edge computing and distributed networks mainly lies heterogeneous clients. For example, heterogeneous clients have different data quality, amount of data, computation capability (i.e., amount of computation resources), communication condition, and willingness to participate.

To improve the performance of model updates, the authors in [9] design a greedy algorithm to find out as many clients with high computation capability and good wireless channel condition as possible. Under bandwidth and time limitation, the authors in [10] design a heuristic algorithm to assign the clients who are willing to upload their local data to a central server. The uploaded data is constructed for approximately independent and identically distributed (i.i.d.), which increases the classification accuracy. In these studies, it is not practical to assume that the clients contribute their resources without the compensation of the cost of consuming resources. Accordingly, the authors in [11], [12], [13] utilize game theory to attract clients to share their resources. In [11], the authors use the Stackelberg game to incentive clients to contribute their data resources for improving the learning accuracy of the model. Similarly, the authors in [12] use the Stackelberg game to incentive clients to contribute their computation resources for reducing the latency of model training. In [13], the authors adopt the Stackelberg game to study the interaction between participating clients and an edge server. The interaction includes the strategies of participating clients and the edge server, i.e., local relative accuracy and reward. The participating clients make optimal local relative accuracy to maximize their benefits. After the edge server makes optimal reward to its benefit, which improves the global accuracy of model training. But the above studies assume that the central server is aware of clients' data qualities, computation capabilities, energy states, and willingness to participate, namely information asymmetry. To overcome the information asymmetry, contract theory is a powerful tool to model the incentive mechanism [15], [16]. The authors in [14] use a multi-weight subjective logic model to design a reputation-based worker selection scheme for reliable federated learning. Then, they use contract theory to stimulate high-reputation workers with high-quality data to participate in model training, which reduces the latency of model training. In addition, a consortium blockchain is used to manage the reputation in a decentralized manner. The above existing work focus on mobile edge computing (MEC) [9], [13] and distributed networks [10], [11], [12], [14]. In this paper, we study federated learning in VEC, which is important for generalizing AI applications in ICV, although it has not been reported in other work. At the same time, we employ two-dimensional contract theory to select some "fine"

TABLE I: A comparison about client selection for federated learning in edge computing and distributed networks.

Ref.	Network Type	Client Heterogeneity	Information Feature	Approach
[9]	Mobile edge computing	Computation capability and communication condition	Information symmetry	Greedy algorithm for selecting clients with high computation capability and good wireless channel condition to improve model performance
[10]	Distributed network	Computation capability and willingness to upload data	Information symmetry	Heuristic algorithm for constructing i.i.d. data to improve model performance
[11]	Distributed network	Amount of data	Information symmetry	Stackelberg game for improving learning accuracy of model
[12]	Distributed network	Computation capability	Information symmetry	Stackelberg Game for reducing latency of model training
[13]	Mobile edge computing	Computation capability and communication condition	Information symmetry	Stackelberg Game for improving global accuracy of model training
[14]	Distributed network	Computation capability	Information asymmetry	Contract based incentive mechanism for reducing latency of model training
This paper	Vehicular edge computing	Image quality and computation capability	Information asymmetry	Two-dimension contract theory for both reducing latency and improving accuracy of model training

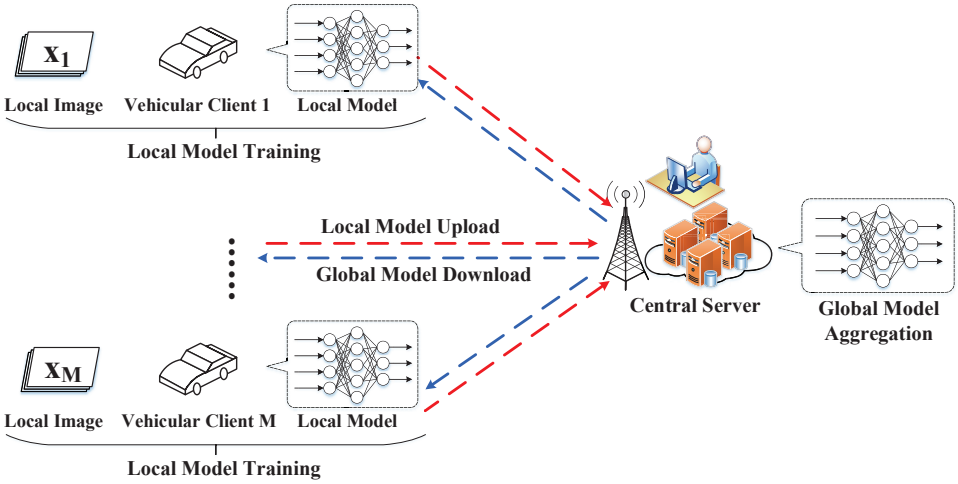

Fig. 1: A general framework of federated learning in vehicular edge computing.

vehicular clients to participate in model aggregation, which reduces latency of model training and improves accuracy of model training. Table I gives the comparison of existing related work and our work.

III. Federated Learning in VEC

In this section, we introduce the wide application of federated learning in VEC by proposing a general framework. We further describe the proposed selective model aggregation approach. The mathematical notations used in this paper are listed in Table II.

A. A General Framework

As shown in Fig. 1, the general framework of federated learning in VEC consists of the following components:

- ***Central Server:*** Central server plays a core role in the procedure of federated learning. It communicates with vehicular clients to collect the updated local DNN models and perform model aggregation. We take image classification as a typical AI application in VEC. DNN-based image classification has been widely used in autopilot and interactive navigation for ICV, as well as object tracking and event detection in ITS [17], [18]. To obtain high accuracy and efficiency of model aggregation, the central server should evaluate the image quality and computation capability of vehicular clients, and select the "fine" models from vehicular clients.
- ***Vehicular Client:*** Vehicular clients are equipped with a set of built-in sensors, such as cameras, GPS, tachographs, lateral acceleration sensors, but also accommodate storage space, computation and communication resources [18]. The built-in sensors are used to capture images. The captured images may be preprocessed for data augment. After that, the preprocessed images are classified and labeled by automatic labeling technology [6], and are cached in vehicular clients. After receiving a request from a central server, vehicular clients separately

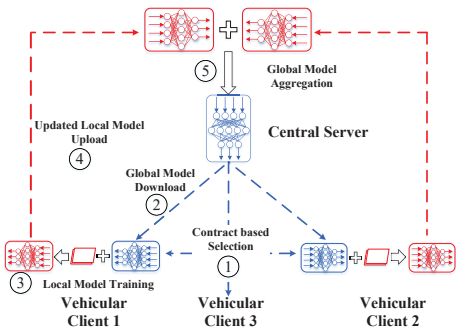

Fig. 2: Selective model aggregation. For a brief introduction, three vehicular clients are illustrated in the case, where vehicular clients 1 and 2 are finally selected while vehicular client 3 is omitted, according to the contract based procedure.

train local DNN models with their own images. Vehicular clients send updated the local DNN models to the central server for model aggregation.

Based on the principle of federated learning, the original federated learning algorithm, i.e., federated averaging (FedAvg), will randomly assign some vehicular clients to perform tasks of training the local DNN models [19]. The selected vehicular clients have diverse image quality and computation capability, which reduces the accuracy and efficiency of model aggregation. To copy with the above dilemma, we propose a selective model aggregation approach.

B. Selective Model Aggregation

As shown in Fig. 2, the main procedure of selective model aggregation has the following steps.

- ***Step 1*: *Contract based selection*** *:* The central server initializes a global DNN model denoted as $\mathbf{w}(0)$. Based on the historical records of vehicular clients, the central server evaluates their image quality and computation capability. The details about the utilized evaluation method are presented in Section IV. Based on the evaluated image quality and computation capability, the central server designs two-dimensional contract items for vehicular clients. Each item includes the amount of image resources, the amount of computation resources and the reward. All the contract items are broadcasted to vehicular clients periodically. The contract items are signed until each type of them is finally accepted by the corresponding type of vehicular clients. For example, vehicular clients 1 and 2 are selected while vehicular client 3 is not, in Fig. 2.
- ***Step 2*: *Global model download*:** After confirming the contract items, vehicular clients 1 and 2 download the global DNN model $\mathbf{w}(0)$ from the central server.
- ***Step 3*: *Local model training*:** According to the predesigned contract items, vehicular clients 1 and 2 train a local DNN model by using their local image and computation resources. More specifically, vehicular client 1 uses the global DNN model $\mathbf{w}(0)$ and a number of x_1 local images to conduct the forward-backward propagation algorithm to minimize the local loss function $F_1(\mathbf{w}(0))$. After E rounds of local iterations, vehicular client 1 updates the local DNN model $\mathbf{w}_1^E(0)$. Similarly, vehicular client 2 updates the local DNN model $\mathbf{w}_2^E(0)$.
- ***Step 4*: *Updated local model upload*:** To meet synchronization requirements, the updated local DNN models $\mathbf{w}_1^E(0)$ and $\mathbf{w}_2^E(0)$, are sent to the central server in time.
- ***Step 5*: *Global model aggregation*:** After receiving the updated local DNN models $\mathbf{w}_1^E(0)$ and $\mathbf{w}_2^E(0)$, the central server aggregates them to update the global DNN model, which generates the global DNN model $\mathbf{w}(1)$. In other words, the central server aggregates the local loss functions $F_1(\mathbf{w}_1^E(0))$ and $F_2(\mathbf{w}_2^E(0))$ as a new global loss function $F(\mathbf{w}(1)) = \frac{x_1 F_1(\mathbf{w}_1^E(0)) + x_2 F_2(\mathbf{w}_2^E(0))}{x_1 + x_2}$ [19].

Steps 1 to 5 form one global iteration (i.e., one communication round). In the k-th global iteration, the change of the global loss function is denoted as $\Delta F_k = F(\mathbf{w}(k)) - F(\mathbf{w}(k-1))$, namely global loss decay similar to [20]. The procedure of selective model aggregation is repeated iteratively until ΔF reaches a predefined threshold.

IV. System Model

We now consider a general scenario where a central server schedules a set of vehicular clients (denoted as M). In the model aggregation, the heterogeneity of resources among the vehicular clients affects the accuracy and efficiency of model aggregation. In other words, the diverse image quality and computation capability affect the accuracy and efficiency of model aggregation, respectively. Each vehicular client knows exactly its image quality and computation capability, but the image quality and computation capability are not available to the central server. This means that there exists asymmetric information between the vehicular clients and the central server. To overcome the above problem, the central server can leverage contract theory to design an incentive mechanism to motivate the vehicular clients to participate in the model aggregation. Because, in contract theory, an employer makes optimal contracts for the employees when the employer does not know the privacy information of each employee [15]. Hence, contract theory is used to model the interactions between the central server and the vehicular clients under information asymmetry. The central server acts as the employer and offers different contract items to the vehicular clients. The vehicular clients act as the employees and select the contract items matching their own types.

Next, we define the image quality and computation capability of vehicular clients. Based on the image quality and computation capability, we model the utilities of the vehicular clients and deduce the types of the vehicular clients. Finally, we model the utility of the central server.

A. Image Quality

Due to the mobility on the roads, the images captured by on-board cameras generally suffer from motion blur, noise, and distortion [21], [22]. The noise and distortion in different vehicular clients may follow identical statistical distribution, while the motion blur level varies with instantaneous velocity

TABLE II: Summary of main notations.

Notation	Definition
ΔF	Global loss decay
$\mathbf{w}_m^E$, $\mathbf{w}$	Local DNN model for vehicular client m and global DNN model
$v^{'}$	Relative velocity between a vehicular client and an object of interest
v_o	Velocity of an object of interest
v	Instantaneous velocity of a vehicular client
σ	Perpendicular distance from the pinhole to the starting point of an object
H	Exposure time interval
s	Camera focal length
δ	Angle between the image plane and the motion direction
l	Length of the motion blur on the image plane
g	Starting position of the object on the image plane
Q	CCD pixel size in the horizontal direction
G	Starting position of position of the object in an image (in pixel)
L	Length of the motion blur in an image (in pixel)
β	Image quality
k	k-th global iteration
M	Number of the vehicular clients
$h(.)$	Revenue function for a vehicular client
p	Reward for a vehicular client
α	Unit cost for collecting image resources
f	The amount of computation resources
x	The amount of image resources
E	The number of local iteration
ι	Unit cost for consuming computation resources
b	Size of each image
η	Effective switched capacitance
ρ	Number of CPU cycles executing one bit
μ	Linear factor for α and e
θ	Type of vehicular client
N	The number of types
ξ	Coefficient determined by specific structure of DNN models
ψ	Unit revenue for the learning efficiency
K	The Number of global iteration
ϕ^d, ϕ^u	Size of global and local DNN model
r^d, r^u	Download and upload data rate

of each vehicular client [7]. For depicting the motion blur level caused by instantaneous velocity, we utilize a geometrical model to illustrate the relationship between an object of interest and the on-board camera. According to the model, the motion blur level can be implicitly predicted by observing the instantaneous velocity of each vehicular client. Referring to [7], we have

$$v' = \frac{\sigma l}{H[s\cos(\delta) - (g+l)\sin(\delta)]}, \tag{1}$$

where v' is the relative velocity between velocity v of vehicular client and velocity v_o of the object, σ is the perpendicular distance from the pinhole to the starting point of an object, l is the length of the motion blur on the image plane, H is the exposure time interval, s is the camera focal length, δ is the angle between the image plane and the motion direction, and g is the starting position of the object on the image plane. We denote the charge-coupled device (CCD) pixel size in the horizontal direction as Q, and have

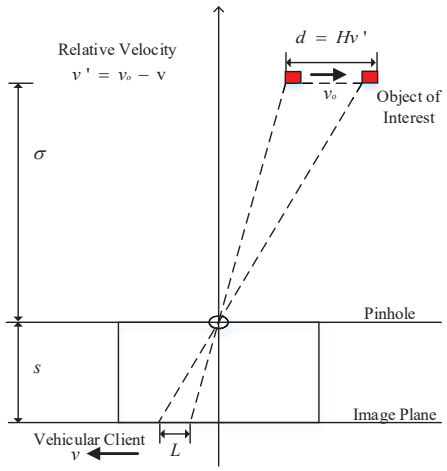

Fig. 3: Geometrical relationship with $\delta = 0$ and $v_o = 0$.

$$L = \frac{v'H\left[s\cos(\delta) - QG\sin(\delta)\right]}{v'HQ\sin(\delta) + \sigma Q}, \tag{2}$$

where G and L are the starting position of the object and the level of motion blur in the image (in pixels), respectively. As shown in Fig. 3, considering the case where the image plane and the motion direction are parallel ($\delta = 0$), and the object of interest is static ($v_o = 0$), Equation (2) is transformed as

$$L = \frac{vsH}{\sigma Q}, \tag{3}$$

where $\frac{sH}{\sigma Q}$ is a parameter of the on-board camera. The equation directly shows that low instantaneous velocity means the low motion blur level.

Based on the motion blur level, we try to evaluate the image quality. Motivated by work [5], we consider that when the motion blur level of training images is more similar to that of testing images, the higher the classifying accuracy is resulted. As a consequence, we measure the image quality by function β that has the form as

$$\beta = \beta(L, L_t), \tag{4}$$

where L_t is the given motion blur level of testing images. Function β has the following characteristics. If L is approximated to L_t, $\beta(L, L_t)$ is larger; and vice versa. If $|L_1 - L_t| = |L_2 - L_t|$ and $L_1 < L_2$, we have $\beta(L_1, L_t) \geq \beta(L_2, L_t)$. To satisfy the above characteristics, $\beta(L, L_t)$ is defined by

$$\beta(L, L_t) = \begin{cases} e^{q_1(L-L_t)}, 0 \leq L \leq L_t, \\ e^{-q_2(L-L_t)}, L_t \leq L, \end{cases} \tag{5}$$

where q_1 and q_2 are two predefined constants. In Fig. 4, we shows an example of function β, where $q_1 = 0.5$, $q_2 = 0.8$ and $L_t = 6$.

In the k-th global iteration, based on the image quality, we express the valuation function of vehicular client m as

$$r_{k,m} = \beta_{k,m} h_k(p_{k,m}), \tag{6}$$

where $\beta_{k,m}$ is the image quality for vehicular client m, $p_{k,m}$ is the reward for contributing image and computation resources

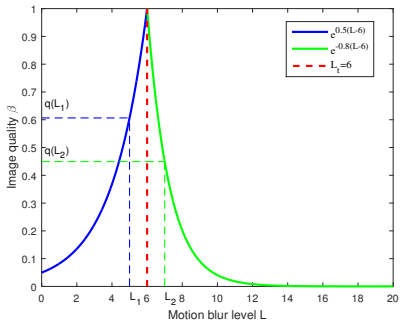

Fig. 4: Image quality with motion blur level.

to the central server, and $h_k(p_{k,m})$ is a revenue function which is increased with the increasing of the reward $p_{k,m}$. The similar valuation function appears in [23].

B. Computation Capability

For vehicular client m, contributing image and computation resources incurs a cost of resource consumption, which is denoted as

$$c_{k,m} = \alpha_{k,m} x_{k,m} + E_{k,m} e_{k,m} x_{k,m} f_{k,m}^2, \tag{7}$$

where $\alpha_{k,m}$ is the unit cost for collecting each image, $x_{k,m}$ is the amount of image resources, and $f_{k,m}$ is the amount of computation resources. E_k is regarded as a constant for all the vehicular clients [14], [24]. According to [25], $e_{k,m} = \iota_{k,m} b_{k,m} \eta_{k,m} \rho_{k,m}$ where $\iota_{k,m}$ is the unit cost for the computation resource consumption, $b_{k,m}$ is the size of each image, $\eta_{k,m}$ is the effective switched capacitance that depends on the chip architecture, and $\rho_{k,m}$ is the number of CPU cycles to process one bit. We consider a special case that $\alpha_{k,m} = \mu_k e_{k,m}$, where μ_k could be identical for all the vehicular clients. So the cost of vehicular client m is simplified into

$$c_{k,m} = \mu_k e_{k,m} x_{k,m} + E_k e_{k,m} x_{k,m} f_{k,m}^2. \tag{8}$$

With the lower $e_{k,m}$, vehicular client m can be more suitable to provide computation resources at a lower cost. Thus, $e_{k,m}$ is denoted as the computation capability of vehicular client m.

C. Utility Function and Type of Vehicular Client

The utility of vehicular client m is related to the difference between its valuation and cost. To sum up (6) and (8), the utility of vehicular client m is shown by

$$u_{k,m} = \beta_{k,m} h_k(p_{k,m}) - \mu_k e_{k,m} x_{k,m} - E_k e_{k,m} x_{k,m} f_{k,m}^2. \tag{9}$$

To formulate the type of vehicular client m, we first transform (9) with a coefficient $e_{k,m}$ as follows

$$\widehat{u_{k,m}} = \frac{u_{k,m}}{e_{k,m}} = \frac{\beta_{k,m}}{e_{k,m}} h_k(p_{k,m}) - \mu_k x_{k,m} - E_k x_{k,m} f_{k,m}^2. \tag{10}$$

The authors in [23] has concluded that the transformation has no impact on contract design. We will also discuss the details later. Thus, the type of vehicular client m is represented by $\theta_{k,m} = \frac{\beta_{k,m}}{e_{k,m}}$.

Definition 1. In the k-th global iteration, the types of vehicular clients are sorted in an ascending order and classified into $\theta_{k,1}, \dots \theta_{k,N}$, which follows

$$\theta_{k,1} < \dots < \theta_{k,n} < \dots < \theta_{k,N}, N \leq M. \tag{11}$$

The higher order of θ implies that they have greater availability to contribute their image and computation resources in the local DNN model training. Each vehicular client can easily determine its own type by measuring its image quality and computation capability while the central server is totally not aware of their exact types. But the central server can obtain the number of each type vehicular clients through observing their historical records. Let $M_{k,n}$ represent the number of vehicular clients belonging to type-n in the k-th global iteration. We have $\sum_{n \in N} M_{k,n} = M_k$. The utility of type-$n$ vehicular client is expressed by

$$\widehat{u_{k,n}} = \theta_{k,n} h_k(p_{k,n}) - c_{k,n}(x_{k,n}, f_{k,n}), \tag{12}$$

where $c_{k,n}(x_{k,n}, f_{k,n}) = \mu_k x_{k,n} + E_k x_{k,n} f_{k,n}^2$.

D. Utility Function of Central Server

In a certain global iteration, the utility of the central server is calculated by

$$U_k = R_k - C_k, \tag{13}$$

where C_k is the cost function in terms of rewards, and R_k is the revenue function in terms of image and computation resources. The revenue function R_k is shown by

$$R_k = \psi_k A_k, \tag{14}$$

where A_k indicates the learning efficiency and ψ_k is the unit revenue for the learning efficiency. According to [20], the learning efficiency is modeled as

$$A_k = \frac{\Delta F_k}{t_k}, \tag{15}$$

where ΔF_k is the global loss decay, and t_k is the end-to-end latency of federated learning in one global iteration.

1) Global Loss Decay: According to [20], vehicular clients contribute more training images for federated learning, which results in a much lower global loss attenuation. Thus, the relationship between the global loss decay and the total amount of contributed training images can be approximately evaluated as

$$\Delta F_k = \xi \sqrt{E_k \sum_{n \in N} M_{k,n} x_{k,n}}, \tag{16}$$

where ξ is the coefficient determined by the specific structure of the DNN model.

2) End-to-End Latency: The central server starts for model aggregation only after receiving all the updated local DNN models. In the k-th global iteration, the end-to-end latency of federated learning for N types is determined by

$$t_k = \max_{n \in N} t_{k,n}, t_k \leq T_k^{max}, \tag{17}$$

where T_k^{max} is the synchronization latency required by the central server and $t_{k,n}$ is the end-to-end latency for type-n vehicular client in the global iteration. The end-to-end latency for type-n vehicular client is calculated by

$$t_{k,n} = t_{k,n}^d + t_{k,n}^c + t_{k,n}^u, \tag{18}$$

where $t_{k,n}^d$ is the latency of downloading the global DNN model, $t_{k,n}^c$ is the latency of training the local DNN model, and $t_{k,n}^u$ is the latency of uploading the updated local DNN model.

- *Global Model Download Latency:* The latency of downloading the global DNN model is

$$t_{k,n}^d = \frac{\phi_{k,n}^d}{r_{k,n}^d}, \tag{19}$$

  where $\phi_{k,n}^d$ is the size of the global DNN model and $r_{k,n}^d$ is the downlink rate.
- *Local Model Training Latency:* Within E_k local iterations, the number of CPU cycles for type-n vehicular client to perform x_n training images, is denoted as $E_k b_{k,n} x_{k,n} \rho_{k,n}$. Thus, the latency of training the local DNN model is

$$t_{k,n}^c = \frac{E_k b_{k,n} x_{k,n} \rho_{k,n}}{f_{k,n}}. \tag{20}$$

- *Updated Local Model Upload Latency:* The latency of uploading the updated local DNN model is given by

$$t_{k,n}^u = \frac{\phi_{k,n}^u}{r_{k,n}^u}, \tag{21}$$

  where $\phi_{k,n}^u$ is the size of the updated local DNN model and $r_{k,n}^u$ is the uplink rate.

For the central server, the cost function C_k is formulated as

$$C_k = \sum_{n \in N} M_{k,n} p_{k,n}. \tag{22}$$

In summary, the entire utility function of the central server is

$$U_k = \frac{\psi_k \xi \sqrt{E_k \sum_{n \in N} M_{k,n} x_{k,n}}}{\max_{n \in N} t_{k,n}(x_{k,n}, f_{k,n})} - \sum_{n \in N} M_{k,n} p_{k,n}. \tag{23}$$

V. Contract Formulation and Solution

To simplify the notations, we skip global iteration k in all the variables below. We first present feasibility conditions overcoming information asymmetry and encouraging the vehicular clients to participate in the model aggregation. Subject to the feasibility conditions, we design a series of two-dimensional contract items to maximize the utility of the central server. The two-dimensional image-computation-reward contract item is denoted as $(x(\theta), f(\theta), p\{x(\theta), f(\theta)\})$ where $x(\theta)$ is the amount of image resources, $f(\theta)$ is the amount of computation resources and $p\{x(\theta), f(\theta)\}$ is the reward for participating in the model aggregation. To simplify expression, the contract item is expressed as (x, f, p). The optimal two-dimensional contract is formulated a non-convex optimization problem. The optimization problem enables each vehicular client to have two kinds of types or two different strategy set. However, it is difficult to optimize two different strategies for each vehicular client simultaneously. In order to solve the dilemma, we relax and simplify the formulated problem into a tractable problem (i.e., one-dimensional adversary selection), where the amount of computation resources relies the amount of image resources. Finally, the tractable problem is solved by a greedy algorithm.

A. Contract Formulation

To encourage the vehicular clients to participate in the model aggregation, the designed contract items need to satisfy the following constraints individual rationality (IR) and incentive compatibility (IC).

Definition 2 (Individual Rationality (IR)). Vehicular clients should choose the contract items ensuring a non-negative utility, i.e.,

$$\begin{aligned} &\widehat{u_n}(x_n, f_n, p_n) = \theta_n h(p_n) - c_n(x_n, f_n) \geq 0, \\ &n \in \{1, 2, \ldots, N\}. \end{aligned} \tag{24}$$

The IR ensures that the reward of each vehicular client compensates the cost of resource consumption in the model aggregation. If $\widehat{u_n} \leq 0$, the vehicular client will not participate in the model aggregation, i.e., choosing the contact item $(x_n = 0, f_n = 0, p_n = 0)$.

Definition 3 (Incentive Compatibility (IC)). Vehicular client m must choose the contract item (x_n, f_n, p_n) matching its own type, which can be mathematically expressed as

$$\begin{aligned} &\theta_n h(p_n) - c_n(x_n, f_n) \geq \theta_n h(p_j) - c_j(x_j, f_j), \\ &n, j, \in \{1, 2, \ldots, N\}. \end{aligned} \tag{25}$$

The IC constraint ensures that each vehicular client automatically chooses the contract items designed for its corresponding type.

With satisfying the constraints of IC and IR, the optimization problem of maximizing the utility of the central server is formulated as

$$\begin{aligned} \max_{(\mathbf{x},\mathbf{f},\mathbf{p})} U &= \frac{\psi \xi \sqrt{E \sum_{n \in N} M_n x_n}}{\max_{n \in N} t_n(x_n, f_n)} - \sum_{n \in N} M_n p_n, \\ \text{s.t. } & C1: \theta_n h(p_n) - c_n(x_n, f_n) \geq 0, n \in \{1, 2, \ldots, N\}, \\ & C2: \theta_n h(p_n) - c_n(x_n, f_n) \geq \theta_n h(p_j) - c_j(x_j, f_j), \\ & n, j \in \{1, 2, \ldots, N\}, \\ & C3: 0 \leq p_n, 0 \leq x_n, 0 < f_n, n \in \{1, 2, \ldots, N\}, \end{aligned} \tag{26}$$

where C1 and C2 are IR and IC, respectively, C3 ensures decision variables are non-negative and $\mathbf{p}, \mathbf{x}, \mathbf{f} \in \mathbb{R}^N$ are vectors.

B. Problem Relaxation and Transformation

1) Relaxing Constraint: It is hard to solve the optimization problem in (26) with non-convex objective function and constraints. To make it better tractable, a new variable T is introduced to denote the end-to-end latency, i.e., $T = \max_{n\in N} t_n(x_n, f_n)$. The optimization problem in (26) is transformed into

$$\begin{aligned}\max_{(\mathbf{x},\mathbf{f},\mathbf{p},T)}\ & U = \frac{\psi\xi\sqrt{E\sum_{n\in N} M_n x_n}}{T} - \sum_{n\in N} M_n p_n,\\ \text{s.t.}\ & C1: \theta_n h(p_n) - c(x_n, f_n) \geq 0, n \in \{1,2,\ldots,N\},\\ & C2: \theta_n h(p_n) - c(x_n, f_n) \geq \theta_n h(p_j) - c(x_j, f_j),\\ & n, j \in \{1,2,\ldots,N\},\\ & C3: 0 \leq p_n, 0 \leq x_n, 0 < f_n, n \in \{1,2,\ldots,N\},\\ & C4: \max_{n\in N} t_n = T,\\ & C5: 0 < T \leq T^{max},\end{aligned} \tag{27}$$

where C5 ensures the end-to-end latency can not achieve the synchronization latency required by the central server.

Lemma 1. *When ρ, b, t^d and t^u are constants with the same value for all vehicular clients, $\max_{n\in N} t_n = T$ is relaxed into $t^d + t^u < T$ and $f_n = \lambda(T)x_n, n \in \{1,2,\ldots,N\}$ where $\lambda(T) = \frac{\rho b E}{(T - t^d - t^u)}$.*

Proof:

$\max_{n\in N} t_n = T$ is firstly relaxed into $t_n = T, n \in \{1,2,\ldots,N\}$. $t_n = T$ is rewritten as $f_n = x_n \frac{\rho_n b_n E}{(T - t_n^d - t_n^u)}$. Referring to [26], [27], ρ_n and b_n are simplified into constants ρ and b with the same value for all vehicular clients. Similar to [14], [24], $\forall n \in N, t_n^d$ and t_n^u are set constants with the same value for all vehicular clients. As a result, $f_n = x_n \frac{\rho_n b_n E}{(T - t_n^d - t_n^u)}$ is simplified into $f_n = x_n \frac{\rho b E}{(T - t^d - t^u)}$. We define $\lambda(T) = \frac{\rho b E}{(T - t^d - t^u)}$ where $T - t^d - t^u > 0$. $f_n = x_n \frac{\rho b E}{(T - t^d - t^u)}$ is rewritten as $f_n = \lambda(T)x_n$ and $t_d + t_u < T$. ∎

To simplify the expression, $\lambda(T)$ is expressed as λ. Replacing $\max_{n\in N} t_n = T$ in (27) with $f_n = \lambda x_n, n \in \{1,2,\ldots,N\}$ and $t_d + t_u < T$, the optimization problem (27) is rewritten as

$$\begin{aligned}\max_{(\mathbf{x},\mathbf{f},\mathbf{p},T)}\ & U = \frac{\psi\xi\sqrt{E\sum_{n\in N} M_n x_n}}{T} - \sum_{n\in N} M_n p_n,\\ \text{s.t.}\ & C1: \theta_n h(p_n) - c_n(f_n, x_n) \geq 0, n \in \{1,2,\ldots,N\},\\ & C2: \theta_n h(p_n) - c_n(f_n, x_n) \geq\\ & \theta_n h(p_j) - c_j(f_j, x_j), n, j \in \{1,2,\ldots,N\},\\ & C3: 0 \leq x_n, 0 < f_n, 0 \leq p_n, n \in \{1,2,\ldots,N\},\\ & C6: f_n = \lambda x_n, n \in \{1,2,\ldots,N\},\\ & C7: t^d + t^u < T \leq T^{max},\end{aligned} \tag{28}$$

where C6 and C7 comes from C4 and C5 with Lemma 1.

By replacing $f_n, n \in \{1,2,\ldots,N\}$ in (28) with $f_n = \lambda x_n, n \in \{1,2,\ldots,N\}$, we can rewrite (28) as

$$\begin{aligned}\max_{(\mathbf{x},\mathbf{p},T)}\ & U = \frac{\psi\xi\sqrt{E\sum_{n\in N} M_n x_n}}{T} - \sum_{n\in N} M_n p_n,\\ \text{s.t.}\ & C1: \theta_n h(p_n) - c_n(\lambda x_n, x_n) \geq 0, n \in \{1,2,\ldots,N\},\\ & C2: \theta_n h(p_n) - c_n(\lambda x_n, x_n) \geq\\ & \theta_n h(p_j) - c_j(\lambda x_j, x_j), n, j \in \{1,2,\ldots,N\},\\ & C3: 0 \leq x_n, 0 \leq p_n, n \in \{1,2,\ldots,N\},\\ & C7: t^d + t^u < T \leq T^{max}.\end{aligned} \tag{29}$$

Using Lemma 1, (x, f, p) is simplified into $(x, \lambda x, p)$, which implies that the amount of computation resources relies the amount of image resources. In other words, for type-n vehicular client, type $\theta_n = \frac{\beta_n}{e_n}$ is simplified into $\theta_n = \frac{\beta_n}{e}$ which only depends the image quality.

2) Simplifying Complicated Constraint: Non-convex and couple constraints in (29), i.e., N IR constraints and $N(N-1)$ IC constraints, makes (29) hard to be solved directly. To reduce constraints of (29), we introduce the following lemmas.

Lemma 2. *Given T, for any feasible contact $(x_n, \lambda x_n, p_n)$, $p_n \geq p_j$ if and only if $x_n \geq x_j, \forall n, j \in \{1,\ldots,N\}$.*

Proof: Please refer to Appendix A. ∎

From Lemma 2, vehicular clients contribute more image resources resulting in more computation resources, the vehicular client will receive more reward. If two vehicular clients contirubte the same amount of image resources, they will recieve the same reward. Using Lemma 2, we can deduce Lemma 3.

Lemma 3 (Monotonicity). *Given T, for any feasible contact $(x_n, \lambda x_n, p_n)$, $p_n \geq p_j$ if and only if $\theta_n \geq \theta_j, \forall n, j \in \{1,\ldots,N\}$.*

Referring to [16], we will finish the following proof.

Proof: Please refer to Appendix B. ∎

Lemma 3 indicates that a higher type vehicular client should get more reward, which is the monotonicity property of the contract design.

Based on the above analysis, the IC constraints are used to reduce the IR constaints. Thus, we have the following lemma.

Lemma 4. *Given T, with the IC condition, the IR constraints can be reduced as*

$$\theta_1 h(p_1) - c_1(\lambda x_1, x_1) \geq 0. \tag{30}$$

Referring to [16], we will finish the following proof.

Proof: Please refer to Appendix C. ∎

Based on the IC constaints, we also have the following lemma.

Lemma 5. *Given T, by utilizing the monotonicity in* **Lemma 3***, the IC condition can be transformed into the Local Downward Incentive Compatibility (LDIC) given by*

$$\begin{aligned}&\theta_n h(p_n) - c_n(\lambda x_n, x_n) \geq \theta_n h(p_{n-1}) - c_{n-1}(\lambda x_{n-1}, x_{n-1}),\\ &n \in \{2, ..., N\},\end{aligned} \tag{31}$$

and the local upward incentive compatibility (LUIC) given by

$$\theta_n h(p_n) - c_n(\lambda x_n, x_n) \geq \theta_n h(p_{n+1}) - c_{n+1}(\lambda x_{n+1}, x_{n+1}), \\ n \in \{1, ..., N-1\}. \tag{32}$$

Referring to [16], we will finish the following proof.

Proof: Please refer to Appendix D. ∎

Using Lemma 2 to Lemma 5, we reduce the complicated IR and IC constraints. The optimization problem in (29) can be further transformed as follows

$$\begin{aligned} \max_{(\mathbf{x},\mathbf{p},T)} U = & \frac{\psi\xi\sqrt{E\sum_{n\in N} M_n x_n}}{T} - \sum_{n\in N} M_n p_n, \\ \text{s.t.} \quad & C1: \theta_n h(p_n) - c_n(\lambda x_n, x_n) \geq 0, n \in \{1,2,\ldots,N\}, \\ & C3: 0 \leq x_n, 0 \leq p_n, n \in \{1,2,\ldots,N\}, \\ & C7: t^d + t^u < T \leq T^{max}, \\ & C8: \theta_n h(p_n) - c_n(\lambda x_n, x_n) \geq \\ & \theta_n h(p_{n-1}) - c_{n-1}(\lambda x_{k,n-1}, x_{k,n-1}), n \in \{2,\ldots,N\}, \\ & C9: \theta_n h(p_n) - c_n(\lambda x_n, x_n) \geq \\ & \theta_n h(p_{n+1}) - c_{n+1}(\lambda x_{n+1}, x_{n+1}), n \in \{1,2,\ldots,N-1\}, \\ & C10: p_1 \leq p_2 \leq \cdots \leq p_N, \end{aligned} \tag{33}$$

where C8 and C9 are the LDIC and LUIC, respectively, and C10 is the monotonicity property of the contract design. Using the LDIC and the LUIC in (33), we can deduce Lemma 6.

Lemma 6. *Given T, since the objective function of (33) is an increasing function in terms of x_n as well as a decreasing function of p_n, $\forall n \in \{1,\ldots,N\}$, the optimization problem in (33) can be further simplified as*

$$\begin{aligned} \max_{(\mathbf{x},\mathbf{p},T)} U = & \frac{\psi\xi\sqrt{E\sum_{n\in N} M_n x_n}}{T} - \sum_{n\in N} M_n p_n, \\ \text{s.t.} \quad & C3: 0 \leq x_n, 0 \leq p_n, n \in \{1,2,\ldots,N\}, \\ & C7: t^d + t^u < T \leq T^{max}, \\ & C10: p_1 \leq p_2 \leq \cdots \leq p_N, \\ & C11: \theta_1 h(p_1) - c_1(\lambda x_1, x_1) = 0, \\ & C12: \theta_n h(p_n) - c_n(\lambda x_n, x_n) = \\ & \theta_n h(p_{n-1}) - c_{n-1}(\lambda x_{n-1}, x_{n-1}), n \in \{2,\ldots,N\}, \end{aligned} \tag{34}$$

where C11 and C12 come from C9 and C10. Referring to [16], we will finish the following proof.

Proof: Please refer to Appendix E. ∎

C. Solution to Optimal Contracts

To quantity the analysis, we consider a case $h(p) = p$. The similar case appears in [26]. We use the method of iterating C11 and C12 constraints to obtain p_n expressed as

$$p_n = \frac{c(x_1, \lambda x_1)}{\theta_1} + \sum\nolimits_{a=1}^{n} \Delta_a, \tag{35}$$

where $\Delta_a = \frac{c(x_a, \lambda x_a)}{\theta_a} - \frac{c(x_{a-1}, \lambda x_{a-1})}{\theta_a}$ and $\Delta_1 = 0$. By replacing p_n in (34) with (35), we can rewrite (34) as

$$\begin{aligned} \max_{(\mathbf{x},T)} U = & \frac{\psi\xi\sqrt{E\sum_{n\in N} M_n x_n}}{T} - \sum_{n\in N} M_n d_n c_n, \\ \text{s.t.} \quad & C3: 0 \leq x_n, n \in \{1,2,\ldots,N\}, \\ & C7: t^d + t^u < T \leq T^{max}, \end{aligned} \tag{36}$$

where $d_n = \frac{M_n}{\theta_n} + \left(\frac{1}{\theta_n} - \frac{1}{\theta_{n+1}}\right)\sum_{j=n+1}^{N} M_j$ with $n < N$, $d_n = \frac{M_n}{\theta_n}$ with $n = N$, and $c_n = \mu x_n + E\lambda^2 x_n^3$.

Given T, it can be easily verified that (36) is a concave optimization problem. Based on the above analysis, we design Algorithm 1. We elaborate the process of Algorithm 1 as follows:

- ***Step 1:*** Initializing parameters such as M, N, E, b, μ, setting $i = 1$, $T = t^u + t^d + \tau$ where τ is a step size, and $U^\star = 0$.
- ***Step 2:*** By solving the optimization problem in (36) with standard convex optimization tools, we get U^i and $\mathbf{x}^i$.
- ***Step 3:*** If $\frac{U^i - U^\star}{U^\star} < 10^{-5}$, the algorithm jumps into step 5; If $U^\star < U^i$, $U^\star$ will be replaced with U^i. Continuously, $i = i + 1$ and $T = T + \tau$ are executed.
- ***Step 4:*** If $T < T^{max}$, the algorithm jumps into step 2. Otherwise, the algorithm returns $U^\star$, $\mathbf{x}^\star$ and $T^\star$.
- ***Step 5:*** Based on the $\mathbf{x}^\star$ and $T^\star$, we compute the optimal price $\mathbf{p}^\star$ and amount of image resources $\mathbf{x}^\star$ with using (35) and amount of computation resources $\mathbf{f} = \lambda(T)\mathbf{x}$, respectively. Finally, the algorithm outputs $\mathbf{p}^\star, \mathbf{x}^\star, \mathbf{f}^\star$ and $T^\star$.

Algorithm 1: Contract Optimization Based Greedy Method

```
Set i = 1, T = t^d + t^u + τ and U* = 0;
while T ≤ T^max do
    Get U^i with solving optimization problem (36) with
     standard convex optimization tools;
    if (U^i − U*)/U* < 10^−5 then
        Break for
    end
    if U* < U_i then
        U* = U_i
    end
    i = i + 1;
    T = T + τ;
end
Return x* and T*;
Assign the optimal price p* with (35) ;
Compute the optimal amount of image resources x* with
  f* = λ(T*)x* ;
Return p*, x*, f*, T*;
```

VI. Numerical Results

A. Simulation Settings

In the simulation, the velocity of vehicular clients is set uniformly distributed in $\left[v^{min}, v^{max}\right]$, where v^{min} and v^{max}

are lower and upper bounds of the velocity, respectively [28]. But the lower and upper bounds are different in urban, suburban, and highway [29]. We consider a suburban case where the velocity of vehicular clients is generated in [0,15] m/s and there are $M = 10$ vehicular clients with $N = 10$ types. By [7], [14], [24], [30], other parameters are listed in Table III. Then, we conduct the simulation in MATLAB to get the optimal contract items. The simulation experiment has two parts.

For the first part, under asymmetric information (CA), we compare the proposed selective model aggregation approach with the original FedAvg approach in terms of accuracy and efficiency of model aggregation. In the FedAvg approach, each vehicular client is supposed to have the same amount of image resources and randomly given computation capability. The simulation involves the public MNIST dataset [31], and the BelgiumTSC (Belgium Traffic Sign for Classification) vehicular dataset [32]. The MNIST dataset consists of $55,000$ training images and $10,000$ testing images of 28×28 pixels. The BelgiumTSC dataset consists of 4591 training images and 2534 testing images. Because the images in the BelgiumTSC dataset are not all the same size, we just resize the images to a fixed size, i.e., 28×28 pixels. The comparison is divided into two cases.

- ***Blurred Training Image and Unblurred Testing Image (BU)***: We randomly divide the training images into 10 groups and each group has the same amount of images. We synthesize motion-blurred images by [33]. The motion blur level is divided into 10 levels, i.e., $L = 1, 2, \ldots, 10$. Each group has a motion blur level. Blurred training images and unblurred testing images constitute the training and testing datasets, respectively.
- ***Blurred Training Image and Blurred Testing Image (BB)***: The training dataset is produced similar to that in BU. The testing images are blurred with level $L = 3$ to constitute the testing dataset.

According to the optimal contract items designed for their own types, each vehicular client picks out a part of training images to train the local DNN model with a convolutional neural network (CNN) in PYTHON. For the MNIST dataset, the local DNN model is executed with iteration round $E = 5$ and full gradient descent. The CNN consists of two convolutional layers followed by two fully connected layers and then another 10 units activated by soft-max, with totally about $1,662,752$ parameters. According to [20], the size of the local DNN model ϕ is about 6.5 MB. For the BelgiumTSC dataset, the local DNN model is executed with iteration round $E = 5$ and full gradient descent. The CNN consists of two convolutional layers followed by three fully connected layers, with totally about $274,730$ parameters. The size of the local DNN model is about 1 MB.

For the second part, we firstly evaluate the optimal contract items in the CA approach. Then, we compare the utilities of the central server and the vehicular clients with existing baseline approaches. The first one is contract based approach under symmetric information (CS). The second one is Stackeberg game based approach under asymmetric information (SG) [12]. The third one is the linear pricing approach [15]. In the SG and the linear pricing approaches, we consider that the unit price for both image resources and computation resources are the same. Finally, we analyze the performance of four approaches under different system settings.

TABLE III: Parameter Setting in the Simulation.

Parameter	**Setting**
CCD pixel size	$Q = 0.011$ mm
Camera focal length	$s = 10$ mm
Perpendicular distance	$\sigma = 5$ m
Exposure time interval	$H = \frac{1}{200}$ s
Effective switched capacitance	$\eta = 10^{-28}$
Number of CPU cycles executing one bit	$\rho = 30$ cycles/bit
Unit cost for consuming computation resources	$\iota = 1$
Coefficient determined by specific structure of DNN models	$\xi = 1$
Download and upload data rate	$r^d = r^u = 6$ MB/s
Unit revenue for the learning efficiency	$\psi = 0.6, 0.8, 1.0$
Linear factor for α and e	$\mu = 5.314 \times 10^{18}$
The number of global iteration	$K = 1000$
The number of local iteration	$E = 3, 4, 5$
Parameters of the image quality	$q_1 = 0.5$, $q_2 = 0.8$, and $L_t = 3$

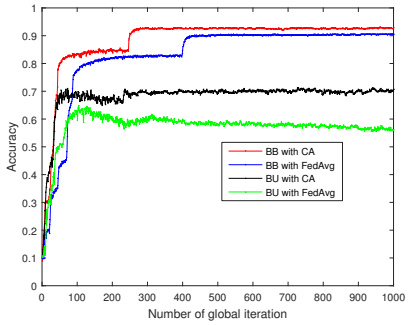

Fig. 5: Accuracy of model aggregation under the MNIST dataset.

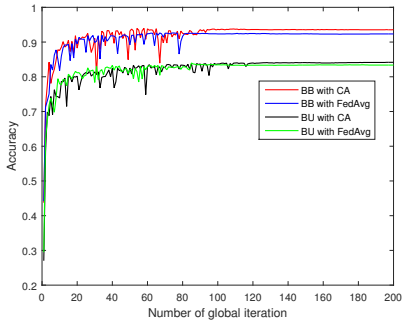

Fig. 6: Accuracy of model aggregation under the BelgiumTSC dataset.

B. Accuracy and Efficiency of Model Aggregation

As shown in Fig. 5, using the MNIST dataset, we compare the accuracy of model aggregation for the CA and FedAvg approaches under BB and BU. As the number of global itera-

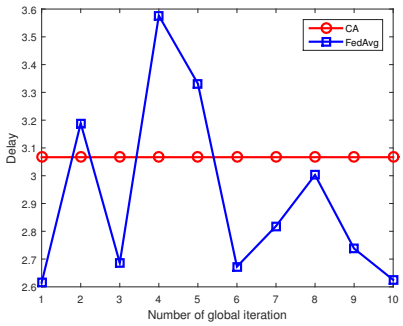

Fig. 7: Efficiency of model aggregation under CA and FedAvg.

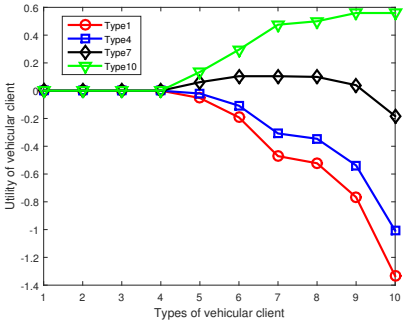

Fig. 8: Utilities of vehicular clients versus types of vehicular clients.

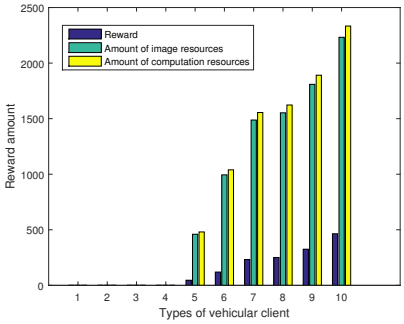

Fig. 9: Contract items with types of vehicular clients.

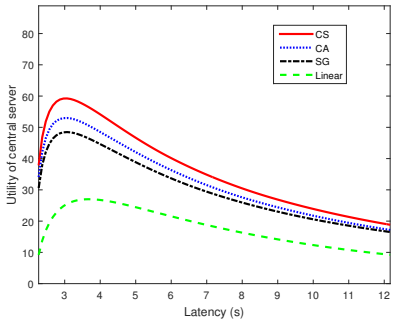

Fig. 10: Utility of central server under different approaches for latency.

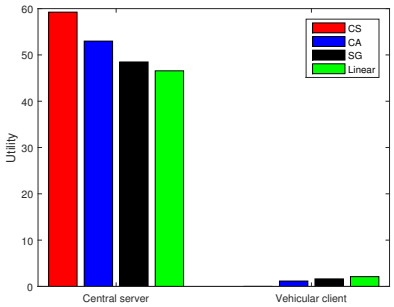

Fig. 11: Utilities of central server and vehicular clients under different approaches.

tion increases, the accuracy of model aggregation is increasing for the BB and BU cases. The accuracy of model aggregation in the BB case is higher than that in the BU case. In the BB case, because the level of training image quality is closer to the level of testing image quality, which causes a high accuracy in classifying the images. In the BU case, because the gap between the level of training image quality and the level of testing image quality is large, which leads to a low accuracy in classifying the images. The similar results appear in [5]. In the BB case, the accuracy of model aggregation with the CA approach is 2.42% higher than the accuracy of model aggregation with the FedAvg approach. In the BU case, the accuracy of model aggregation adopting the CA approach is 6.28% higher than the accuracy of model aggregation adopting the FedAvg approach.

As shown in Fig. 6, using the BelgiumTSC dataset, we also compare the accuracy of model aggregation for the CA and FedAvg approaches under BB and BU. The accuracy of model aggregation in the BB case is also higher than that in the BU case. In the BB case, the accuracy of model aggregation with the CA approach is 1.23% higher than that of the FedAvg approach. In the BU case, the accuracy of model aggregation adopting the CA approach is 0.2% higher than that of the FedAvg approach.

For the CA and FedAvg approaches in the MNIST dataset, Fig. 7 shows the efficiency of model aggregation for global iteration number $k = 1, 2, \ldots, 10$. Since the FedAvg approach is not adapted to the random computation capability in the vehicular clients, the training latency changes in a wide range, which causes inefficient model aggregation. In the CA approach, the synchronization of training latency is beneficial for the model aggregation. The performance of efficiency of the model aggregation in the BelgiumTSC dataset has similar results to that in the MNIST.

C. Optimal Contract Analysis

The IR and IC constraints are verified in Fig. 8. It shows the utilities of type-1, type-4, type-7 and type-10 vehicular clients. The central server offers all the contract items $(p_n, x_n, f_n), n \in 1, 2, \ldots, N$ for each vehicular client. Fig. 8 shows the utility of each vehicular client is maximized when choosing the contract item designed for its own type, which

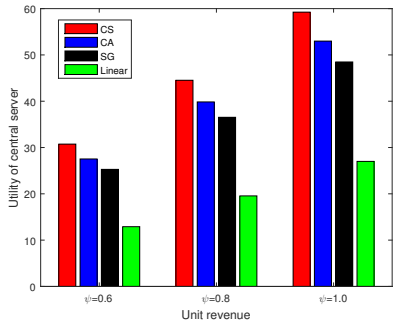

Fig. 12: Utility of central server under different approaches with unit revenue.

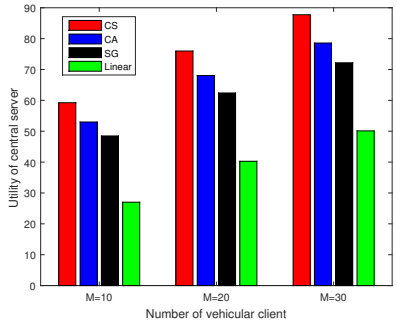

Fig. 13: Utility of central server under different approaches for number of vehicular clients.

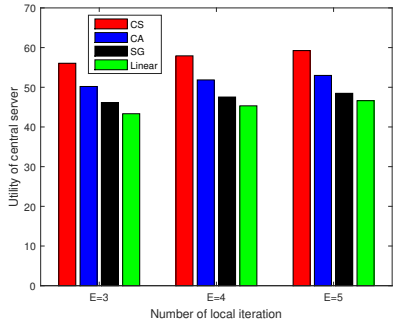

Fig. 14: Utility of central server under different approaches with number of local iteration.

means satisfying the IC constraint. For instance, we focus on the utility of type-7 vehicular client. If type-7 vehicular client chooses the contract item (p_7, x_7, f_7) fitting its corresponding type, the utility of type-7 vehicular client could be maximized. If type-7 vehicular client chooses any other contract item $(p_j, x_j, f_j), n \in 1, 2, \ldots, N, j \neq 7$, the utility of type-7 vehicular client can not be maximized compared with the contract item (p_7, x_7, f_7). Furthermore, when each vehicular client selects the contract item fitting its corresponding type, the utility of each vehicular client is nonnegative, which indicates that the IR constraint is satisfied. Therefore, after choosing the best contract item designed for its own type, the types of the vehicular clients will be revealed to the central server. In other words, by applying the proposed approach, the central server can be aware of the image quality and computation capability of the vehicular clients.

Fig. 9 shows that the contract items under different types of the vehicular clients. The contract item includes the amount of image resources, the amount of computation resources and the reward. To show contract items in the same figure, the amount of computation resources and the reward are reduced by 10^7 times and 10^2 times, respectively. The relationship among contract items remains unchanged. As the type becomes higher, each type of vehicular client is eager to share more image and computation resources, which leads to higher reward. This means Lemma 2 and Lemma 3 are both satisfied.

Fig. 10 shows the effect of latency T on the utility of the central server under four approaches, i.e., CS, CA, SG, and linear pricing approaches. For four approaches, as the latency grows, the utility of the central server first increases to the maximum value and then decreases. With a given latency, firstly, the CS approach achieves the best performance among four approaches and serves as upper bound. It is because that the central server is fully aware of the types of the vehicular clients, tries its best to extract the revenue from the vehicular clients until the utilities of all the vehicular clients are zeros. Secondly, two contract based approaches (CS and CA) have more the utility of the central server than the SG approach. Since the contract based approaches try to extract the revenue from the vehicular clients as much as possible while satisfying both the IR and IC constraints, which leads to leave less revenue for the vehicular clients. However, the SG approach aims at maximizing both the utilities of the central server and the vehicular clients, which can reserve more revenue for the vehicular clients. Finally, the utility of the central server achieved by the SG approach is better than the linear pricing approach. In other words, the linear pricing approach achieves the worst performance among four approaches and serves as lower bound. It is because that the linear pricing approach can't allow the central server to adopt to the change of the amount of image resources and computation resources, and make the performance become worse.

D. System Parameter Analysis

With optimal latency, Fig. 11 compares the utilities of the vehicular clients and the central server for adopting four approaches. For the central server, the performance among four approaches is similar to Fig. 10. For the vehicular clients, firstly, the best performance of the vehicular clients is the linear pricing approach as upper bound while the worst performance of the vehicular clients is the CS approach as lower bound. Secondly, the performance of the vehicular clients by adopting the CA approach and the SG approach is between the upper and lower bound. Furthermore, the SG approach gets higher utilities of the vehicular clients than the CA approach. The reason can be referred to Fig. 10.

For four approaches, Fig. 12 shows the utility of the central server under different unit revenue. As the unit revenue increases, the utility of the central server is also increasing. It is because that the utility of the central server increases linearly with ψ. With a fixed unit revenue, the performance

of the central server under four approaches is similar to Fig. 10. Fig. 13 compares the effect of the number of vehicular clients on the utility of the central server for adopting four approaches. For four approaches, as the number of vehicular clients increases, the utility of the central server is also increasing. It is because that the utility of the central server increases with M. For a given number M, the performance of the central server under four approaches is similar to Fig. 10.

Fig. 14 shows the relationship between the number of local iterations and the utility of the central server under four approaches. With the increasing of the number of local iteration, the utility of the central server is also increasing. It is noted that the objective function in (36) shows the high number of local iterations increases the global loss decay while increasing the cost of the reward. Probably because the increasing rate of the global loss decay exceeds the increasing rate of the cost of the reward. As a result, the utility of the central server gradually increases. With a given local iterations E, the performance of the central server under four approaches is similar to Fig. 10.

VII. Conclusion

In this paper, we study selective model aggregation of image classification for federated learning in vehicular edge computing. Using the geometric relationship between the object of interest and the camera motion in vehicular clients, we first evaluate the image quality in the motion blur level. To select out the "fine" local DNN models with satisfying image quality and computation capability, the model selection procedure is formulated as a two-dimensional image-computation-reward contract-theoretic problem. The contract problem is transformed into a tractable problem through relaxing and simplifying the complicated constraints, and eventually solved by a greedy algorithm. Extensive simulation is conducted to demonstrate the performance enhancement of the proposed approach in terms of model accuracy and aggregation efficiency.

Appendix A
Proof of the Lemma 2

We bring the $f_n = \lambda x_n$ into the $c_n(x_n, f_n)$ given by

$$c_n(x_n, \lambda x_n) = \mu x_n + E\lambda^2 x_n^3. \tag{37}$$

It is obvious that $c_n(x_n, \lambda x_n)$ is a convex function in terms of x_n. To simplify the expression, $c_n(x_n, \lambda x_n)$ is expressed as c_n. First, we prove that if $x_n > x_j$, then $p_n > p_j$. According to constraint (25), we have the following inequality:

$$c_n - c_j < \theta_n(h(p_n) - h(p_j)), n, j \in N. \tag{38}$$

Since $x_n > x_j$, we can obtain $c_n - c_j > 0$. Then, $h(p_n) - h(p_j) > 0$ is satisfied. Due to the increasing valuation function of $h(\cdot)$, we have $p_i > p_j$. Furthermore, we prove that if $p_n > p_j$, then $\theta_n > \theta_j$. Referring to constraint (25), we have the following inequality:

$$\theta_j(h(p_n) - h(p_j)) < c_n - c_j, n, j \in N. \tag{39}$$

Since $p_i > p_j$ and $h(\cdot)$ is a monotonically increasing valuation function in terms of p, we have $\theta_j(h(p_n) - h(p_j)) > 0$. Thus, we can obtain $c_n - c_j$, i.e., $x_n > x_j$. Finally, we prove that $x_n = x_j$ if and only if $p_n = p_j$, $\forall n, j \in \{1, ..., N\}$. We use the similar procedure to prove $x_n = x_j$ if and only if $p_n = p_j$.

Appendix B
Proof of the Lemma 3

First, we prove the sufficiency: if $\theta_n \geq \theta_j$, then $p_n \geq p_j$. Based on the IC constraints of type θ_n and type θ_j vehicular clients, we have

$$\theta_n h(p_n) - c_n \geq \theta_n h(p_j) - c_j, \tag{40}$$

and

$$\theta_j h_j - c_j \geq \theta_j h(p_n) - c(x_n). \tag{41}$$

Adding (40) and (41), and by rearranging, we can get $(\theta_n - \theta_j)(h(p_n) - h(p_j)) \geq 0$. As $\theta_n \geq \theta_j$, we must have $h(p_n) - h(p_j) \geq 0$. Since $p_n \geq p_j$ and $h(\cdot)$ is a monotonically increasing valuation function in terms of p, we have $p_n \geq p_j$. Next, we prove the necessity: if $p_n \geq p_j$, then $\theta_n \geq \theta_j$. Similar to the above process, we use the IC constraint to obtain the same result $(\theta_n - \theta_j)(h(p_n) - h(p_j)) \geq 0$. The reason is similar to the sufficiency.

Appendix C
Proof of the Lemma 4

Given that $\theta_1 < \theta_2 < ... < \theta_N$, we utilize IC constraints to have

$$\theta_n h(p_n) - c_n \geq \theta_n h(p_1) - c_1 \geq \theta_1 h(p_1) - c_1 \geq 0. \tag{42}$$

(42) indicates that the first type of vehicular client satisfies the IR constraint, other types of vehicular clients will satisfy the other IR constraints automatically. Thus, we need to keep the IR constraint for the first type and the other IR constraints can be reduced.

Appendix D
Proof of the Lemma 5

The IC constraints between types *n* and *j*, $n, j \in \{2, ..., N\}$ are defined as downward incentive constraints (DICs) represented as

$$\theta_n h(p_n) - c_n \geq \theta_n h(p_j) - c_j, \ \forall n, j \in \{2, ..., N\}, n > j. \tag{43}$$

The IC constraints between type *n* and type *j*, $n, j \in \{2, ..., N\}$ are defined as upward incentive constraints (UICs) represented as

$$\theta_n h(p_n) - c_n \geq \theta_n h(p_j) - c_j, \ \forall n, j \in \{2, ..., N\}, n < j. \tag{44}$$

Specifically, two adjacent types in UICs are defined as LUICs and two adjacent types in DICs are defined as LDICs. The LUICs and LDICs can be represented as, respectively,

$$\theta_n h(p_n) - c_n \geq \theta_n h(p_{n+1}) - c_{n+1}, \ \forall n \in \{1, ..., N-1\}, \tag{45}$$

and

$$\theta_n h(p_n) - c_n \geq \theta_n h(p_{n-1}) - c_{n-1}, \ \forall n \in \{2, ..., N\}. \tag{46}$$

With the following proof, we will first reduce the DIC to the LDIC. Adopting the LDIC with three continuous types of the vehicular clients, $\theta_{n-1} \leq \theta_n \leq \theta_{n+1}, n \in \{2, ..., N-1\}$, we have the following inequalities

$$\theta_{n+1}h(p_{n+1}) - c_{n+1} \geq \theta_{n+1}h(p_n) - c_n, \tag{47}$$

$$\theta_n h(p_n) - c_n \geq \theta_n h(p_{n-1}) - c_{n-1}. \tag{48}$$

According to the monotonicity, i.e., $p_n > p_j$ if and only if $\theta_n > \theta_j$, we have

$$\theta_{n+1}(h(p_n) - h(p_{n-1})) \geq \theta_n(h(p_n) - h(p_{n-1})). \tag{49}$$

Combining (48) and (49), we have

$$\theta_{n+1}h(p_n) - c_n \geq \theta_{n+1}h(p_{n-1}) - c_{n-1}. \tag{50}$$

Combining (47) and (50), we have

$$\theta_{n+1}h(p_{n+1}) - c_{n+1} \geq \theta_{n+1}h(p_{n-1}) - c_{n-1}. \tag{51}$$

Using (51), we can prove that all the DICs can hold

$$\begin{aligned}\theta_{n+1}h(p_{n+1}) - c_{n+1} \geq \theta_{n+1}h(p_{n-1}) - c_{n-1} \geq ... \\ \geq \theta_{n+1}h(p_1) - c_1.\end{aligned} \tag{52}$$

Hence, we use the LDICs to hold and reduce all the DICs. Using similar process, we can also prove that all the UICs can automatically hold, when the LUICs are satisfied.

APPENDIX E
PROOF OF THE LEMMA 6

We will first prove that the reduced IR constraint $\theta_1 h(p_1) - c_1 \geq 0$ can be reduced to $\theta_1 h(p_1) - c_1 = 0$. For the reduced IR constraint, the data requester will try its best to decrease p_1 to improve the optimization objective function U until $\theta_1 h(p_1) - c_1 = 0$.

Secondly, we will prove that the LDIC can be transformed as $\theta_n h(p_n) - c_n = \theta_n h(p_{n-1}) - c_{n-1}$, which is combined with monotonicity to ensure the LUIC hold. Notice that the LDIC $\theta_n h(p_n) - c_n \geq \theta_n h(p_{n-1}) - c_{n-1},\ \forall n \in \{2, ..., N\}$ will still hold if both p_n and p_{n-1} are reduced to the same amount. To maximize the optimization objective function, the data requester will decrease p_j as possible as it can until $\theta_n h(p_n) - c_n = \theta_n h(p_{n-1}) - c_{n-1}$. Notice that this process doesn't have an effect on other types LDIC. So the LDIC can be simplified as $\theta_n h(p_n) - c_n = \theta_n h(p_{n-1}) - c_{n-1}, \forall n \in \{2, ..., N\}$.

Thirdly, we will prove that if $\theta_n h(p_n) - c_n = \theta_n h(p_{n-1}) - c_{n-1}, \forall n \in \{2, ..., N\}$ and the monotonicity hold, the LUIC holds. The constraint $\theta_n h(p_n) - c_n = \theta_n h(p_{n-1}) - c_{n-1}, \forall n \in \{2, ..., N\}$ can be transformed as

$$\theta_n h(p_n) - \theta_n h(p_{n-1}) = c_n - c_{n-1}. \tag{53}$$

Due to the monotonicity, i.e., if $\theta_n \geq \theta_{n-1}$, then $h(p_n) \geq h(p_{n-1})$, we further have

$$\theta_n h(p_n) - \theta_n h(p_{n-1}) \geq \theta_{n-1}h(p_n) - \theta_{n-1}h(p_{n-1}). \tag{54}$$

Combine (53) and (54), we have

$$\begin{aligned}\theta_n h(p_n) - \theta_n h(p_{n-1}) = c_n - c_{n-1} \\ \geq \theta_{n-1}h(p_n) - \theta_{n-1}h(p_{n-1}).\end{aligned} \tag{55}$$

Equation (55) equally is transformed as

$$\theta_{n-1}h(p_{n-1}) - c_{n-1} \geq \theta_{n-1}h(p_n) - c_n, \tag{56}$$

which is exactly the LUIC condition. So we remove the LUIC from the constraints in (34).

REFERENCES

[1] Q. Yang, Y. Liu, T. Chen, and Y. Tong, "Federated machine learning: Concept and applications," *ACM Transactions on Intelligent Systems and Technology (TIST)*, vol. 10, no. 2, pp. 12:1–12:19, February 2019.

[2] A. Hard, K. Rao, R. Mathews, F. Beaufays, S. Augenstein, H. Eichner, C. Kiddon, and D. Ramage, "Federated learning for mobile keyboard prediction," 2018. [Online]. Available: https://arxiv.org/abs/1811.03604 .

[3] T. S. Brisimi, R. Chen, T. Mela, A. Olshevsky, I. C. Paschalidis, and W. Shi, "Federated learning of predictive models from federated electronic health records," *International journal of medical informatics*, vol. 112, pp. 59–67, April 2018.

[4] L. Liu, C. Chen, Q. Pei, S. Maharjan, and Y. Zhang, "Vehicular edge computing and networking: A survey," 2019. [Online]. Available: https://arxiv.org/abs/1908.06849

[5] Y. Pei, Y. Huang, Q. Zou, H. Zang, X. Zhang, and S. Wang, "Effects of image degradations to cnn-based image classification," 2018. [Online]. Available: https://arxiv.org/abs/1810.05552.

[6] P. Dube, B. Bhattacharjee, S. Huo, P. Watson, and B. Belgodere, "Automatic labeling of data for transfer learning," in *IEEE Conference on Computer Vision and Pattern Recognition (CVPR) Workshops*, Long Beach, CA, June 2019, pp. 122–129.

[7] J. A. Cortés-Osorio, J. B. Gómez-Mendoza, and J. C. Riaño-Rojas, "Velocity estimation from a single linear motion blurred image using discrete cosine transform," *IEEE Transactions on Instrumentation and Measurement*, vol. 68, no. 10, pp. 4038–4050, October 2019.

[8] W. Y. B. Lim, N. C. Luong, D. T. Hoang, Y. Jiao, Y.-C. Liang, Q. Yang, D. Niyato, and C. Miao, "Federated learning in mobile edge networks: A comprehensive survey," 2019. [Online]. Available: https://arxiv.org/abs/1909.11875

[9] T. Nishio and R. Yonetani, "Client selection for federated learning with heterogeneous resources in mobile edge," in *IEEE International Conference on Communications (ICC)*, Shanghai, China, May 2019, pp. 1-7.

[10] N. Yoshida, T. Nishio, M. Morikura, K. Yamamoto, and R. Yonetani, "Hybrid-fl: Cooperative learning mechanism using non-iid data in wireless networks," 2019. [Online]. Available: https://arxiv.org/abs/1905.07210

[11] S. Feng, D. Niyato, P. Wang, D. I. Kim, and Y.-C. Liang, "Joint service pricing and cooperative relay communication for federated learning," in *Proceedings of the International Conference on Internet of Things (iThings) and IEEE Green Computing and Communications (GreenCom) and IEEE Cyber, Physical and Social Computing (CPSCom) and IEEE Smart Data (SmartData)*, Atlanta, GA, USA, July 2019, pp. 815-820.

[12] Y. Sarikaya and O. Ercetin, "Motivating workers in federated learning: A stackelberg game perspective," *IEEE Networking Letters*, 2019, to be published, DOI: 10.1109/LNET.2019.2947144.

[13] S. R. Pandey, N. H. Tran, M. Bennis, Y. K. Tun, A. Manzoor, and C. S. Hong, "A crowdsourcing framework for on-device federated learning," 2019. [Online]. Available: https://arxiv.org/abs/1911.01046

[14] J. Kang, Z. Xiong, D. Niyato, S. Xie, and J. Zhang, "Incentive mechanism for reliable federated learning: A joint optimization approach to combining reputation and contract theory," *IEEE Internet of Things Journal*, 2019, to be published, DOI: 10.1109/JIOT.2019.2940820.

[15] Y. Zhang, L. Liu, Y. Gu, D. Niyato, M. Pan, and Z. Han, "Offloading in software defined network at edge with information asymmetry: A contract theoretical approach," *Journal of Signal Processing Systems*, vol. 83, no. 2, pp. 241–253, May 2016.
[16] Z. Hou, H. Chen, Y. Li, and B. Vucetic, "Incentive mechanism design for wireless energy harvesting-based internet of things," *IEEE Internet of Things Journal*, vol. 5, no. 4, pp. 2620–2632, August 2018.
[17] Y. Jing, B. Guo, Z. Wang, V. O. Li, J. C. Lam, and Z. Yu, "Crowdtracker: Optimized urban moving object tracking using mobile crowd sensing," *IEEE Internet of Things Journal*, vol. 5, no. 5, pp. 3452–3463, October 2018.
[18] D. Yang, K. Jiang, D. Zhao, C. Yu, Z. Cao, S. Xie, Z. Xiao, X. Jiao, S. Wang, and K. Zhang, "Intelligent and connected vehicles: Current status and future perspectives," *Science China Technological Sciences*, vol. 61, no. 10, pp. 1446–1471, October 2018.
[19] H. B. McMahan, E. Moore, D. Ramage, S. Hampson, and B. A. y Arcas, "Communication-efficient learning of deep networks from decentralized data," in *Proceedings of the International Conference on Artificial Intelligence and Statistics (AISTATS)*, Fort Lauderdale, FL, USA, April 2017, pp. 1273–1282.
[20] J. Ren, G. Yu, and G. Ding, "Accelerating dnn training in wireless federated edge learning system," 2019. [Online]. Available: https://arxiv.org/abs/1905.09712
[21] S. Dodge and L. Karam, "Understanding how image quality affects deep neural networks," in *eighth IEEE international conference on quality of multimedia experience (QoMEX)*, Lisbon, Portugal, June 2016, pp. 1–6.
[22] S. Ghosh, R. Shet, P. Amon, A. Hutter, and A. Kaup, "Robustness of deep convolutional neural networks for image degradations," in *IEEE International Conference on Acoustics, Speech and Signal Processing (ICASSP)*, Calgary, AB, Canada, April 2018, pp. 2916–2920.
[23] Y. Chen, S. He, F. Hou, Z. Shi, and J. Chen, "An efficient incentive mechanism for device-to-device multicast communication in cellular networks," *IEEE Transactions on Wireless Communications*, vol. 17, no. 12, pp. 7922–7935, December 2018.
[24] N. H. Tran, W. Bao, A. Zomaya, and C. S. Hong, "Federated learning over wireless networks: Optimization model design and analysis," in *IEEE Conference on Computer Communications*, Paris, France, April 2019, pp. 1387–1395.
[25] Y. Wang, M. Sheng, X. Wang, L. Wang, and J. Li, "Mobile-edge computing: Partial computation offloading using dynamic voltage scaling," *IEEE Transactions on Communications*, vol. 64, no. 10, pp. 4268–4282, August 2016.
[26] C. Li, S. Wang, X. Huang, X. Li, R. Yu, and F. Zhao, "Parked vehicular computing for energy-efficient internet of vehicles: A contract theoretic approach," *IEEE Internet of Things Journal*, vol. 6, no. 4, pp. 6079–6088, August 2019.
[27] S. Wang, X. Huang, R. Yu, Y. Zhang, and E. Hossain, "Permissioned blockchain for efficient and secure resource sharing in vehicular edge computing," 2019. [Online]. Available: https://arxiv.org/abs/1906.06319
[28] T. Zhang, R. E. De Grande, and A. Boukerche, "Vehicular cloud: Stochastic analysis of computing resources in a road segment," in *Proceedings of the 12th ACM Symposium on Performance Evaluation of Wireless Ad Hoc, Sensor, & Ubiquitous Networks*, New York, NY, USA, November 2015, pp. 9-16.
[29] A. F. Molisch, F. Tufvesson, J. Karedal, and C. F. Mecklenbrauker, "A survey on vehicle-to-vehicle propagation channels," *IEEE Wireless Communications*, vol. 16, no. 6, pp. 12–22, December 2009.
[30] H.-Y. Lin, K.-J. Li, and C.-H. Chang, "Vehicle speed detection from a single motion blurred image," *Image and Vision Computing*, vol. 26, no. 10, pp. 1327–1337, October 2008.
[31] Y. LeCun and C. Cortes, "MNIST handwritten digit database," 2010. [Online]. Available: http://yann.lecun.com/exdb/mnist/
[32] R. Timofte, K. Zimmermann, and L. Van Gool, "Multi-view traffic sign detection, recognition, and 3d localisation," *Machine Vision and Applications*, vol. 25, no. 3, pp. 633–647, April 2014.
[33] J. Sun, W. Cao, Z. Xu, and J. Ponce, "Learning a convolutional neural network for non-uniform motion blur removal," in *Proceedings of the IEEE Conference on Computer Vision and Pattern Recognition*, Boston, MA, USA, June 2015, pp. 769–777.

Dongdong Ye received the M.S. degree in 2018 from the Guangdong University of Technology, Guangzhou, China, where he is currently working toward the Ph.D. degree. His research interests mainly focus on game theory, resource management in wireless communications and networking, and data sharing and trading.

Rong Yu (M'08) received his B.S. degree in Communication Engineering from Beijing University of Posts and Telecommunications, China, in 2002 and Ph.D. degree in Electronic Engineering from Tsinghua University, China, in 2007, respectively. After that, he worked in the School of Electronic and Information Engineering at South China University of Technology. In 2010, he joined the School of Automation at Guangdong University of Technology, where he is currently a Professor. His research interests include wireless networking and mobile computing such as mobile cloud, edge computing, deep learning, connected vehicles, smart grid and Internet of Things. He is the author or co-author of over 100 international journal and conference papers and the co-inventor of over 50 patents in China. He was a member of the Home Networking Standard Committee in China, where he led the standardization work of three standards.

Miao Pan (S'07-M'12-SM'18) received his BSc degree in Electrical Engineering from Dalian University of Technology, China, in 2004, MASc degree in electrical and computer engineering from Beijing University of Posts and Telecommunications, China, in 2007 and Ph.D. degree in Electrical and Computer Engineering from the University of Florida in 2012, respectively. He is now an Associate Professor in the Department of Electrical and Computer Engineering at University of Houston. He was a recipient of NSF CAREER Award in 2014. His research interests include cybersecurity, deep learning privacy, big data privacy, cyber-physical systems, and cognitive radio networks. His work won IEEE TCGCC (Technical Committee on Green Communications and Computing) Best Conference Paper Awards 2019, and Best Paper Awards in ICC 2019, VTC 2018, Globecom 2017 and Globecom 2015, respectively. Dr. Pan is an Associate Editor for IEEE Internet of Things (IoT) Journal from 2015 to 2018. He has also been serving as a Technical Organizing Committee for several conferences such as TPC Co-Chair for Mobiquitous 2019, ACM WUWNet 2019. He is a member of ACM and a senior member of IEEE.

Zhu Han (S'01-M'04-SM'09-F'14) received the B.S. degree in electronic engineering from Tsinghua University, in 1997, and the M.S. and Ph.D. degrees in electrical and computer engineering from the University of Maryland, College Park, in 1999 and 2003, respectively. From 2000 to 2002, he was an R&D Engineer of JDSU, Germantown, Maryland. From 2003 to 2006, he was a Research Associate at the University of Maryland. From 2006 to 2008, he was an assistant professor at Boise State University, Idaho. Currently, he is a John and Rebecca Moores Professor in the Electrical and Computer Engineering Department as well as in the Computer Science Department at the University of Houston, Texas. He is also a Chair professor in National Chiao Tung University, ROC. His research interests include wireless resource allocation and management, wireless communications and networking, game theory, big data analysis, security, and smart grid. Dr. Han received an NSF Career Award in 2010, the Fred W. Ellersick Prize of the IEEE Communication Society in 2011, the EURASIP Best Paper Award for the Journal on Advances in Signal Processing in 2015, IEEE Leonard G. Abraham Prize in the field of Communications Systems (best paper award in IEEE JSAC) in 2016, and several best paper awards in IEEE conferences. Dr. Han was an IEEE Communications Society Distinguished Lecturer from 2015-2018, and is AAAS fellow since 2019 and ACM distinguished Member since 2019. Dr. Han is 1% highly cited researcher since 2017 according to Web of Science.